

# Fe<sub>3</sub>O<sub>4</sub> Core/Layered Double Hydroxide Shell Nanocomposite: Versatile Magnetic Matrix for Anionic Functional Materials\*\*

Liang Li,\* Yingjun Feng, Yongsheng Li, Wenru Zhao, and Jianlin Shi\*

Recently, micro- or nanospheres with magnetic cores and functional shell structures have received much attention because of their potential applications in catalysis, drug storage/release, selective separation, chromatography, and chemical or biosensors.<sup>[1–10]</sup> Until now, different shell frameworks have been developed to pursue these aims. Some groups fabricated mesoporous silica shell to load metal oxides and fluorescence imaging materials and used them in catalysis and drug storage/release systems.<sup>[1–3]</sup> Diat et al. discovered that monodisperse and compactly packed onion phases could be obtained in concentrated solutions of surfactants under controlled mechanical shear. Their applications as carriers for drug delivery or nanoreactors for the synthesis of metal nanoparticles have been explored.<sup>[8]</sup> Wang et al. used dimer-captosuccinimide acid modified Fe<sub>2</sub>O<sub>3</sub> nanoparticles and combined them with CdSe/ZnS quantum dots (QDs) to prepare water soluble magnetic luminescent composites in an organic/water two-phase mixture.<sup>[9]</sup> Bawendi and co-workers simultaneously encapsulated both CdSe QDs and  $\gamma$ -Fe<sub>2</sub>O<sub>3</sub> in silica microspheres to prepare a magnetic luminescent composite.<sup>[10]</sup> All these exploitations of the shell structure greatly expand the realm of applications of magnetic core/shell materials. However, in all of these applications, the method for loading functional materials into the shell structure is largely different from each other, even for the same shell structures. Is there a facile and versatile approach to synthesize magnetic core/functional shell structures?

Layered double hydroxides (LDHs), consisting of stacked brucite-type octahedral layers with anions and water molecules occupying the interlayer space, are currently attracting intense research interest.<sup>[11–13]</sup> Recently, we succeeded in total delamination of LDH crystals in nitrate form upon treatment with formamide, and used this product as a building block to

fabricate the LDH hollow shell structure.<sup>[14]</sup> The LDH structure collapsed upon heat treatment at about 500 °C to yield mixed oxides of constituent elements, which underwent restoration of the LDH structure in the presence of water and anions.<sup>[15]</sup> This so-called memory effect property of LDHs has been employed as an effective synthetic route for inserting various functional inorganic and organic anions into LDHs galleries.<sup>[16,17]</sup>

Herein, we report the synthesis and characterization of a Fe<sub>3</sub>O<sub>4</sub> core/oxide shell nanocomposite decomposed from a layered double hydroxide, which combines both versatile anion loading capability and high separation efficiency, making it an ideal support for recoverable anionic functional materials. As shown in Figure 1, the center of the structure is a

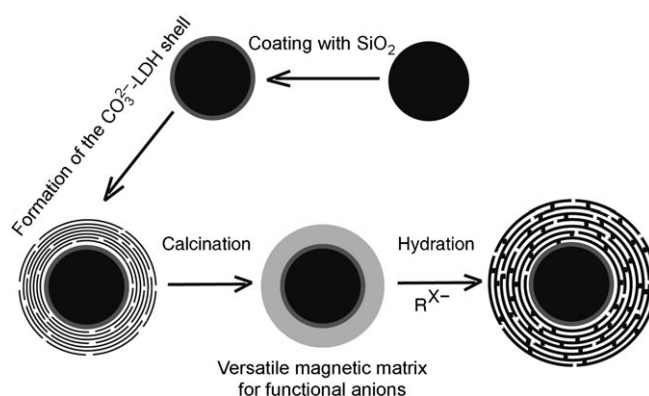


**Figure 1.** Synthesis of the magnetic core/anionic functionalized LDH shell composite structure. The Fe<sub>3</sub>O<sub>4</sub> core is first coated with a thin layer of silica, then further coated with a multilayer CO<sub>3</sub><sup>2–</sup>–LDH composite shell. Afterwards, a calcination process is performed to remove CO<sub>3</sub><sup>2–</sup>, and the shell become amorphous. Finally, the LDH structure can be restored and anions can be simultaneously intercalated in between the LDH galleries upon immersion in an aqueous solution containing the desired anions.

silica-coated magnetite (Fe<sub>3</sub>O<sub>4</sub>) core, which is composed of many small Fe<sub>3</sub>O<sub>4</sub> crystallites. The Fe<sub>3</sub>O<sub>4</sub> cores strongly interact with external magnetic fields and can be easily separated from solution under a moderate magnetic field. The outer surface of the structure is layered double hydroxide. It can be expected that recoverable anionic functional materials will be easily formed through the reconstruction of this thermally decomposed Fe<sub>3</sub>O<sub>4</sub> core/LDH shell composite.

Mg–Al LDH powder (mole ratio Mg/Al = 3:1) in carbonate form was obtained from Kyowa Chemical Industry Co., Ltd. Mg–Al LDH was converted into a nitrate form by anion exchange in a typical salt/acid treatment, and subsequently

[\*] Prof. Dr. L. Li, Dr. Y. Feng, Dr. Y. Li, Dr. W. Zhao, Prof. Dr. J. Shi  
Key Laboratory for Ultrafine Materials of Ministry of Education,  
School of Materials Science and Engineering, East China University  
of Science and Technology, Shanghai 200237 (China)  
Fax: (+86) 21-6425-0740  
E-mail: liliang@ecust.edu.cn

Prof. Dr. J. Shi  
State Laboratory of High Performance Ceramic and Superfine  
Microstructure, Shanghai Institute of Ceramics, Chinese Academy  
of Sciences, Shanghai 200050 (China)  
E-mail: jlshi@sunm.shcnc.ac.cn

[\*\*] This work was supported by the National Nature Foundation of China (grant no. 20633090), Shanghai Pujiang Program (grant no. 08PJ14035), and Shanghai Nature Science Foundation (grant no. 07ZR14028).

Supporting information for this article is available on the WWW under <http://dx.doi.org/10.1002/anie.200901730>.

delaminated in formamide.<sup>[14a]</sup> A typical synthetic procedure of versatile magnetic matrix for anionic functional materials is as follows. Magnetic  $\text{Fe}_3\text{O}_4$  crystalline particles (ca. 400 nm) were synthesized using a solvent-thermal method.<sup>[18]</sup> After being coated by a layer of silica following a sol-gel process reported previously by Shi et al.,<sup>[3]</sup> silica-coated magnetite core composites (0.5 g) were dispersed in a formamide suspension (100 mL) containing LDH nanosheets (0.05 g) and then ultrasonically agitated for 20 minutes to promote the adsorption of LDH nanosheets onto the silica surface. The sample was recovered by centrifugation (6000 rpm, 10 min) and washed with ultrapure water. In the next step, the sample was redispersed in an aqueous solution of  $\text{Na}_2\text{CO}_3$  (100 mL,  $2\text{ g L}^{-1}$ ). The product was recovered by centrifugation.  $\text{Fe}_3\text{O}_4/\text{SiO}_2$  cores coated with 20 layer pairs of carbonate and LDH nanosheets ( $(\text{CO}_3^{2-}/\text{LDH})_{20}$ ) were synthesized by repeating the above procedures 20 times. The obtained sample was heated to  $480^\circ\text{C}$  at a ramp rate of  $20^\circ\text{C h}^{-1}$  under  $\text{N}_2$  atmosphere and kept at this temperature for 4 h to remove  $\text{CO}_3^{2-}$  and water. Finally, the calcined material was dispersed into aqueous solution to recover its original LDH structure and in the meantime absorb the functional anions into the LDH galleries.

Figure 2 depicts X-ray diffraction (XRD) data for the sample at various stages of the fabrication of  $\text{Fe}_3\text{O}_4$  core/LDH shell nanocomposite. Characteristic peaks from the  $\text{Fe}_3\text{O}_4$

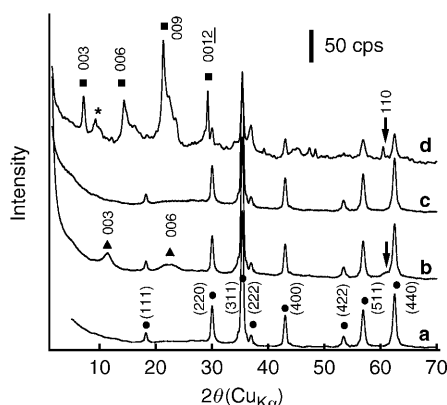


**Figure 2.** XRD patterns of  $\text{Fe}_3\text{O}_4$  core alone (a); after deposition of 20  $\text{LDH}/\text{CO}_3^{2-}$  layer pairs (b); after calcination at  $480^\circ\text{C}$  for 4 h (c); and after treatment in  $\text{W}_7\text{O}_{24}^{6-}$  aqueous solution (d). (Diffraction peaks of  $\bullet$ :  $\text{Fe}_3\text{O}_4$ ;  $\blacktriangle$ : carbonate-LDH;  $\blacksquare$ :  $\text{W}_7\text{O}_{24}^{6-}$ -LDH;  $*$ : polyoxometalate-LDH).

core in an angular range of  $18\text{--}65^\circ$  remained intact during the complete process. The sample coated with 20 layer pairs of LDH nanosheets/ $\text{CO}_3^{2-}$  shows two major peaks at  $2\theta$  values of  $11.3$  and  $22.7^\circ$  (indicated by triangles), which can be ascribed to the formation of carbonate LDH shell nanostructure with a repeating distance of approximately  $0.78\text{ nm}$ ; a similar value has been reported many times for carbonate LDH in power form.<sup>[19]</sup> One additional new peak at  $60.5^\circ$  can be assigned to intrasheet reflections of 110 peaks from a two-dimensional hexagonal cell ( $a = 0.31\text{ nm}$ ),<sup>[20]</sup> confirming that

the LDH nanosheet architecture remained intact in the layer-by-layer assembly process.

This kind of LDH core/shell structure possesses versatile anion loading capability after calcination because of its memory effect, which makes them ideal supports for recoverable anionic functional materials. Herein, we chose  $\text{W}_7\text{O}_{24}^{6-}$  as an example and investigated the photodegradation behavior of aqueous organochlorine pesticide by using this  $\text{Fe}_3\text{O}_4$  core/ $\text{W}_7\text{O}_{24}^{6-}$  LDH as a model system to demonstrate the use of our core/shell structure as a versatile recoverable catalyst support.

The original carbonate LDH shell structure was destroyed after heating at  $480^\circ\text{C}$  under  $\text{N}_2$  atmosphere for 4 h. The XRD pattern (Figure 2c) does not show any peak other than that from the  $\text{Fe}_3\text{O}_4$  core, suggesting the transformation of the LDH shell to amorphous metal oxides such as  $\text{MgO}$  and  $\text{Al}_2\text{O}_3$ . When this  $\text{Fe}_3\text{O}_4$  core/amorphous shell material was dispersed into the prepared aqueous solution at  $50^\circ\text{C}$  to absorb the  $\text{W}_7\text{O}_{24}^{6-}$  for 24 h, the sample became crystalline again (Figure 2d). The four major peaks (at  $2\theta$  values of  $7.2^\circ$ ,  $14.5^\circ$ ,  $21.6^\circ$ , and  $29.0^\circ$ ) can be ascribed to a basal diffraction series with an interplanar spacing of  $1.2\text{ nm}$ . The additional peak at  $60.5^\circ$  can be identified as two-dimensional diffraction peaks of the 110 plane for a hexagonal cell with  $a = 0.31\text{ nm}$ . The XRD data strongly suggest an anion inserting process and reconstruction of the LDH structure by the layer memory effect. The basal spacing of  $1.2\text{ nm}$  is characteristic of LDHs in  $\text{W}_7\text{O}_{24}^{6-}$  form.<sup>[17]</sup> Furthermore, compared with the original calcined sample, there is also a broad diffraction peak around a  $2\theta$  value of  $10^\circ$  (indicated by the asterisk), which is the fingerprint of polyoxometalates pillared LDH.<sup>[20]</sup> This result is further confirmation that  $\text{W}_7\text{O}_{24}^{6-}$  ions have been successfully inserted into the LDH gallery. In addition, the average shell thickness of the reconstructed  $\text{Fe}_3\text{O}_4$  core/ $\text{W}_7\text{O}_{24}^{6-}$  LDH shell composite is calculated by using Sherrer's equation on the (003) peak to be around  $20\text{ nm}$ .

Figure 3c shows a scanning electron microscopy (SEM) image of the obtained  $\text{Fe}_3\text{O}_4/\text{SiO}_2$  core/ $\text{CO}_3^{2-}$  LDH shell composite. The spherical morphology of monodisperse  $\text{Fe}_3\text{O}_4$  core/silica shell beads was preserved well after the deposition of the 20 layers of carbonate LDH shell. The LDH nanosheets can rarely be identified in SEM images because of their high flexibility. The only noticeable difference between the spheres with or without shells was the surface roughness. The spherical morphology was well preserved and there is no visible unwrapped core or separate irregular particles in the SEM image. The  $\text{CO}_3^{2-}$ -LDH shell thickness is estimated from Figure 3d to around  $15\text{ nm}$ .

When calcined at  $480^\circ\text{C}$ , the  $\text{Fe}_3\text{O}_4$  core/carbonate shell sample lost  $4.2\%$  of its weight in two steps (Figure 4). These weight losses were accompanied by huge endothermic peaks, suggesting the decomposition of the carbonate LDH shell. The endothermic peak at  $214^\circ\text{C}$  can be assigned to dehydration of the carbonate LDH layer, and two peaks at about  $320^\circ\text{C}$  and  $412^\circ\text{C}$  can be assigned as dehydroxylation or the collapse of the hydroxide layers, which overlaps the decomposition of  $\text{CO}_3^{2-}$  to  $\text{CO}_2$ , as shown in Figure 5. These data are consistent with those in the literature.<sup>[18]</sup> Slow heating at a rate of  $2^\circ\text{C min}^{-1}$  was essential to retain the shell structure. Rapid

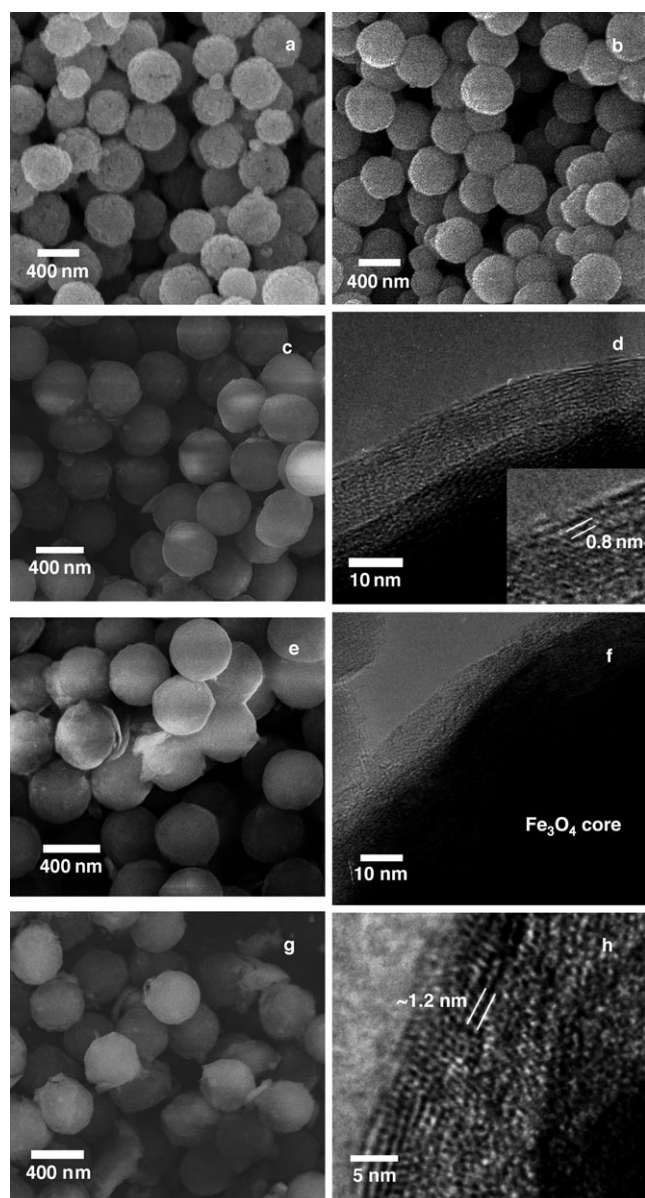


**Figure 3.** SEM images of  $\text{Fe}_3\text{O}_4$  core (a),  $\text{Fe}_3\text{O}_4$  core covered with  $\text{SiO}_2$  layer (b),  $\text{Fe}_3\text{O}_4/\text{SiO}_2$  core/ $\text{CO}_3^{2-}$ -LDH shell composite (c), the core shell structure after calcination (e), and the  $\text{Fe}_3\text{O}_4/\text{SiO}_2$  core/ $\text{W}_7\text{O}_{24}^{6-}$ -LDH shell structure after reconstruction (g); TEM images of  $\text{Fe}_3\text{O}_4/\text{SiO}_2$  core/carbonate LDH shell composite (d), the core shell structure after calcination (f), and  $\text{Fe}_3\text{O}_4/\text{SiO}_2$  core/ $\text{W}_7\text{O}_{24}^{6-}$ -LDH shell structure after reconstruction (h).

heating of the sample could disrupt the shell structure as a result of violent evolution of steam and carbon dioxide.

The FTIR data shown in Figure 5 are additional evidence for the chemical and structural modifications of the sample described above. The as-prepared silica covered  $\text{Fe}_3\text{O}_4$  core/carbonate LDH shell nanocomposite showed sharp adsorption bands attributable to  $\text{CO}_3^{2-}$  and  $\text{SiO}_2$ . A strong peak at  $1350\text{ cm}^{-1}$  can be assigned as a vibration mode of carbonate ions and a peak at  $1090\text{ cm}^{-1}$  can be assigned as a stretching mode of Si-O-Si, indicating the formation of carbonate LDH shell on the surface of  $\text{Fe}_3\text{O}_4/\text{SiO}_2$  core after the layer-by-layer

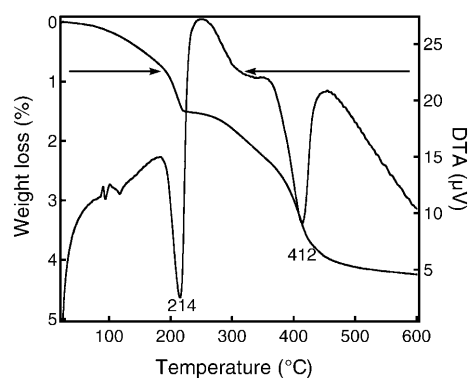


**Figure 4.** Thermogravimetry/differential thermal analysis (TG-DTA) diagram of  $\text{Fe}_3\text{O}_4$  core/carbonate LDH shell composite.

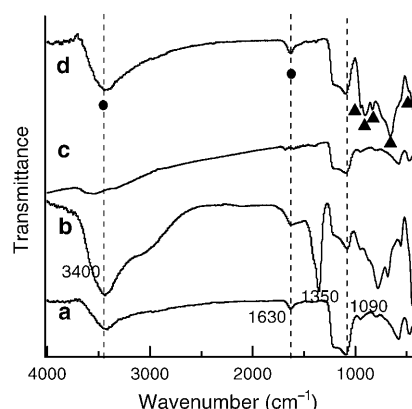


**Figure 5.** FTIR spectra of  $\text{Fe}_3\text{O}_4/\text{SiO}_2$  core initially (a), after layer-by-layer coating with carbonate LDH (b), after calcination at  $480^\circ\text{C}$  for 4 h (c), and after reconstruction in  $\text{W}_7\text{O}_{24}^{6-}$  aqueous solution (d). ●: adsorption bands of water molecules; ▲:  $\text{W}_7\text{O}_{24}^{6-}$  ions.

process. In addition to these peaks, there were strong adsorption bands at  $3700\text{--}3000$  and at  $1630\text{ cm}^{-1}$ , which are attributable to the stretching and bending vibrations of water molecules. This result suggests that the LDH/ $\text{CO}_3^{2-}$  shell has been hydrated. In contrast, the spectrum of the calcined sample was rather featureless as a consequence of the removal of interlayer ions and the collapse of LDH layers. The reconstruction of the LDH structure after mixing with the  $\text{W}_7\text{O}_{24}^{6-}$  aqueous solution is clear from the bands at  $3400$  and  $1630\text{ cm}^{-1}$  (labeled with black dots). Furthermore, some additional peaks at  $950$ ,  $905$ ,  $833$ ,  $661$ , and  $581\text{ cm}^{-1}$  (indicated by triangles) appeared. All these bands can be ascribed to the vibration mode of  $\text{W}_7\text{O}_{24}^{6-}$  ions,<sup>[17]</sup> again indicating the formation of LDH in  $\text{W}_7\text{O}_{24}^{6-}$  form.

After the shell structure recovered from the amorphous metal oxides to the LDH structure, the spherical morphology is still apparent (Figure 3e,f). Compared with the sample before reconstruction, the shell thickness became somewhat larger and the surface became rougher. The high-resolution TEM (HRTEM) image shows a lamellar structure with a repeating fringe of  $1.2\text{ nm}$  (Figure 3h), and a shell thickness about  $20\text{ nm}$ , which is consistent with the XRD results.



The content of  $\text{W}_7\text{O}_{24}^{6-}$  in the resulting catalyst is about 8.0 wt %, as determined by chemical analysis. The activity of this magnetic recoverable catalyst was tested with the photodegradation of trace hexachlorocyclohexane (HCH) in aqueous solution (Figure 6). After the suspension was stirred in the

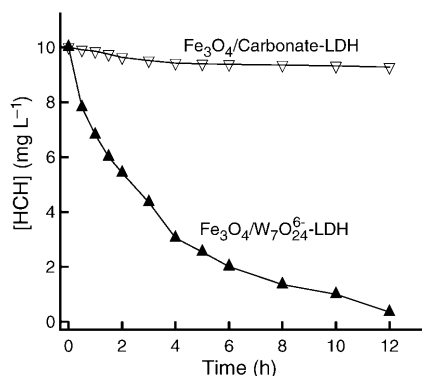


**Figure 6.** Mineralization of HCH as a function of irradiation time in the presence of magnetic  $\text{W}_7\text{O}_{24}^{6-}$  catalyst.

dark for 12 h or irradiated with a high pressure mercury lamp (HPML) for 12 h in the absence of catalyst, there was no apparent change in the concentration of HCH, and  $\text{Cl}^-$  and  $\text{CO}_2$  were not detected. However, a significant transformation of HCH into  $\text{Cl}^-$  and  $\text{CO}_2$  was observed after irradiating the suspension containing synthesized catalyst with the HPML. In the reaction system, the concentration of the product  $\text{Cl}^-$  ions increased with the reaction time, suggesting that the degradation of aqueous HCH was the result of photoexcited catalysis rather than direct photolysis. Complete mineralization of HCH was demonstrated by 96.3% chlorine recovered as  $\text{Cl}^-$  for 10  $\text{mg L}^{-1}$  HCH after 12 h irradiation of the suspension. Photocatalytic activity was not observed with the  $\text{Fe}_3\text{O}_4$  core/carbonate LDH shell nanocomposite. The magnetic separation and recycling of the catalyst were also investigated with the same reaction (Figure 7). The catalyst could be effectively recycled and reused six times without any apparent decrease in its catalytic activity (Table 1). This catalyst also shows high catalytic activities in oxidative

**Table 1:** Magnetic separation and recycling of the catalyst in the photodegradation of HCH.

| Cycle                         | 1    | 2    | 3    | 4    | 5    | 6    |
|-------------------------------|------|------|------|------|------|------|
| Yield [%] of photodegradation | 96.3 | 95.8 | 96.1 | 96.5 | 95.6 | 96.4 |

alkoxylation of mesitol with various alcohols (see the Supporting Information).<sup>[21–23]</sup>

In summary, we have demonstrated the fabrication of magnetic core/LDH shell structure and its use as recoverable support for nanocatalysts. This composite structure possesses high anion loading capacity and can be conveniently separated. The success in the assembly of the  $\text{W}_7\text{O}_{24}^{6-}$  catalyst may provide a general route to the facile and direct fabrication of magnetic core/various anion-functionalized shell composite structures. The magnetic nanocomposite catalyst system demonstrated herein is expected to find many important applications in catalysis. For example, the oxide shell could be used as an absorbent to carry anionic drugs and used in a drug storage/release system.

## Experimental Section

X-ray diffraction (XRD) data were collected using a Rigaku Rint-2000 powder diffractometer with graphite monochromated Cu KR radiation ( $\lambda = 0.15405 \text{ nm}$ ). Transmission electron microscopy (TEM) observations were performed on a field emission JEM-3000F (JEOL) electron microscope operated at 300 kV equipped with a Gatan-666 electron energy loss spectrometer and energy-dispersive X-ray spectrometer. Scanning electron microscopy (SEM) images were obtained using a JEOL JSM-6700F electron microscope (accelerating voltage of 10 kV). FTIR spectra were obtained on Nicolet 7000-C spectrometer.

**Photocatalytic procedure:** The temperature of the system was maintained at 28°C. The light source was a 125 W high-pressure mercury lamp. A general photocatalytic procedure was carried out as follows. The  $\text{Fe}_3\text{O}_4$  core/layered double hydroxide shell nanocomposite (0.5 g) were suspended in a fresh aqueous solution of HCH. The suspension was ultrasonicated for 5 min, stirred in the dark for 30 min, and then irradiated with the lamp. The suspension was vigorously stirred during the irradiation process.

Received: March 31, 2009

Revised: May 20, 2009

Published online: July 2, 2009

**Keywords:** heterogeneous catalysis · layered materials · magnetic properties · nanostructures

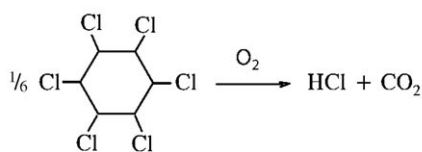


**Figure 7.** Photodegradation of HCH and magnetic separation of the catalyst.

- [1] M. Shokouhimehr, Y. Piao, Y. Kim, Y. Jang, T. Hyeon, *Angew. Chem.* **2007**, *119*, 7169–7173; *Angew. Chem. Int. Ed.* **2007**, *46*, 7039–7043.
- [2] J. Kim, H. S. Kim, N. Lee, T. Kim, H. Kim, T. Ku, I. C. Song, W. K. Moon, T. Hyeon, *Angew. Chem.* **2008**, *120*, 8566–8569; *Angew. Chem. Int. Ed.* **2008**, *47*, 8438–8441.
- [3] W. Zhao, J. Gu, L. Zhang, H. Chen, J. Shi, *J. Am. Chem. Soc.* **2005**, *127*, 8916–8917.
- [4] H. Zhao, J. F. Chen, Y. Zhao, L. Jiang, J. W. Sun and J. Yun, *Adv. Mater.* **2008**, *20*, 3682–3686.
- [5] X. Hong, J. Li, M. Wang, J. Xu, W. Guo, J. Li, Y. Bai, T. Li, *Chem. Mater.* **2004**, *16*, 4022–4027.
- [6] J. Ge, T. Huynh, Y. Hu, Y. Yin, *Nano Lett.* **2008**, *8*, 931–934.

- [7] E. V. Shevchenko, M. I. Bodnarchuk, M. V. Kovalenko, D. V. Talapin, R. K. Smith, S. Aloni, W. Heiss, A. P. Alivisatos, *Adv. Mater.* **2008**, *20*, 4323–4329.
- [8] O. Diat, D. Roux, F. Nallet, *J. Phys. II* **1993**, *3*, 1427–1452.
- [9] D. Wang, J. He, N. Rosenzweig, Z. Rosenzweig, *Nano Lett.* **2004**, *4*, 409–413.
- [10] N. Insin, J. B. Tracy, H. Lee, J. P. Zimmer, R. M. Westervelt, M. G. Bawendi, *ACS Nano* **2008**, *2*, 197–202.
- [11] B. Sels, D. De Vos, M. Buntinx, F. Pierard, A. K. Mesmaeker, P. Jacobs, *Nature* **1999**, *400*, 855–857.
- [12] J.-H. Choy, J.-M. Oh, M. Park, K.-M. Sohn, J.-W. Kim, *Adv. Mater.* **2004**, *16*, 1181–1184.
- [13] M. Darder, M. López-Blanco, P. Aranda, F. Leroux, E. Ruiz-Hitzky, *Chem. Mater.* **2005**, *17*, 1969–1977.
- [14] a) L. Li, R. Ma, Y. Ebina, N. Iyi, T. Sasaki, *Chem. Mater.* **2005**, *17*, 4386–4391; b) L. Li, R. Ma, N. Iyi, Y. Ebina, K. Takada, T. Sasaki, *Chem. Commun.* **2006**, 3125–3127.
- [15] S. Miyata, *Clays Clay Miner.* **1980**, *28*, 50–55.
- [16] T. Hibino, A. Tsunashima, *Chem. Mater.* **1998**, *10*, 4055–4061.
- [17] Y. Guo, D. Li, C. Hu, Y. Wang, E. Wang, Y. Zhou, S. Feng, *Appl. Catal. B* **2001**, *30*, 337–349.
- [18] H. Deng, X. Li, Q. Peng, X. Wang, J. Chen, Y. Li, *Angew. Chem.* **2005**, *117*, 2842–2845; *Angew. Chem. Int. Ed.* **2005**, *44*, 2782–2785.
- [19] *Handbook of Layered Materials* (Eds.: S. M. Auerbach, K. A. Carrado, P. K. Dutta), Marcel Dekker, New York, **2004**.
- [20] *Intercalation Chemistry* (Eds.: M. S. Whittingham, A. J. Jacobson), Academic Press, New York, **1982**.
- [21] B. F. Sels, D. E. De Vos, P. A. Jacobs, *J. Am. Chem. Soc.* **2007**, *129*, 6916–6926.
- [22] B. F. Sels, D. E. De Vos, M. Buntinx, P. A. Jacobs, *J. Catal.* **2003**, *216*, 288–297.
- [23] B. F. Sels, D. E. De Vos, P. A. Jacobs, *Angew. Chem.* **2005**, *117*, 314–317; *Angew. Chem. Int. Ed.* **2005**, *44*, 310–313.